

METHODICAL DEVELOPMENT OF A STRUCTURAL HEALTH MONITORING SYSTEM FOR COPV SUPPORTED BY A DIGITAL SHADOW

Rebecca Richstein^{1*}, Thorsten Reichartz¹, Andreas Janetzko-Preisler¹, Kai-Uwe Schröder¹

¹RWTH Aachen University, Institute of Structural Mechanics and Lightweight Design,
Wüllnerstraße 7, 52062 Aachen, Germany

* rebecca.richstein@sla.rwth-aachen.de

Key words: Structural Health Monitoring, Digital Shadow, COPV

Summary: *The need for safe storage of hydrogen by pressurized vessel will increase, due to their good performance in terms of weight and pressurisation, Composite Overwrapped Pressure Vessels (COPV) are promising candidates for the storage of hydrogen. However, damages in fibre composite materials such as delaminations often cannot be detected by visual inspection. Using a Structural Health Monitoring (SHM) system, changes in the structural integrity can be determined and further correlated to damages. This approach supports a safe use and an appropriate service life of COPVs. This paper proposes a strain-based SHM approach which uses a previously generated damage database. The database is reduced to a few measurement points, so information is only available at potential sensor locations. For damage detection and assessment new virtual data sets, representing measurements, are compared pairwise with these pre-calculated database taking into account a potential fuzziness. The developed algorithm showed good results with regard to damage detection within the conducted tests. If a damage case is already stored in the database, it will be exactly identified. Even unknown damage that is similar to a database entry can be assessed by the algorithm.*

1 INTRODUCTION

In order to reduce greenhouse gas emissions and thus mitigate the effects of climate change, the automotive industry is increasingly focusing on the use of renewable energies and drive technologies. Next to the battery as an energy storage device, the fuel cell is the biggest competing technology. It is estimated that the share of fuel cell-powered vehicles for the public and freight sector will amount up to 50% in 2040 [1]. Therefore, the need for safe storage of hydrogen by pressurized vessel will increase. Due to their good performance in terms of weight and pressurisation, Composite Overwrapped Pressure Vessels (COPV) are a promising candidate for the storage of hydrogen COPVs consist of a metal or plastic liner to ensure impermeability, and a covering overwrap of carbon fibre which provides the necessary strength for pressurisation of the vessel. [2] However, structures made of fibre composite material have more complex failure mechanisms than structures made of isotropic materials. Therefore, COPVs must be regularly inspected, for example with non-destructive testing (NDT). [3] NDT can be utilized as a recertification method for maintenance issues, such as visual inspection, ultrasonic C-scan, acoustic emission, shearography, eddy current, X-ray and thermography [4]. Despite the fact that these NDT methods offer numerous possibilities for examining

components, these methods are still time-consuming and require expensive equipment. Therefore, the idea of condition-based maintenance is becoming highly interesting for COPV. With an online Structural Health Monitoring (SHM) system, the performance changes of COPV can be determined and further translated into damage. This allows weight reductions and cost savings without compromising safety [5]. Just like NDT, SHM has a variety of measurement techniques, such as vibration-based, acoustic emission, strain, etc., to monitor composite structure [6]. In the following part of the paper, a strain-based approach is used, which will be further explained in the text. Many strain-based approaches using Fibre Optical Sensors (FOS) over the whole COPV to measure a complete strain distribution. However, for cost reasons, it would be reasonable to reduce the number of measuring points and only measure at a limited number of discrete points. Since measured values are only recorded at a limited discrete number of points, the database or the model must also be reduced to discrete measuring points. In the following, the reduction of the overall model to a few representative measuring points is referred to as a Digital Shadow. This designation becomes particularly important when coupled with a real counterpart, which has not been done in the context of this paper.

In this paper SHM methods applied to COPVs are reviewed at first. In the next step the model and the model reduction approach is presented and applied to the COPV. Afterwards, the functioning of the derived SHM system is described and analysed.

2 CURRENT SHM METHODS FOR COPV MONITORING

As discussed in the introduction, there are many different approaches for SHM with regard to measurement techniques: e.g. guided waves, acoustic emission, vibration or strain-based methods. Along with each method different sensor technologies are available [6]. An example for the application of the guided waves for COPV approach is given by McKeon [3]. He investigated the propagation of ultrasonic guided waves within an experimental. Thereby the experimental setup allows detecting impact damages and is recommended for further application.

Vibration-based SHM technology is also proposed as a method for the monitoring of COPVs. Zhou et al. [7] used modal properties and dynamic response to detect the damage on a non-pressurized composite fuel tank. Bocian et al. [8] used modal tests and FEM simulations to investigate the possibilities for damage detection. It was proven that damage induced by impact has a noticeable influence on natural frequencies, and thus the modal analysis seems to be a useful tool for impact detection in COPV.

Different SHM methods can also be combined. Huang and Schröder [9] proposed a hybrid between vibration and strain based methods, by combining a static strain monitoring with the mode shape curvature node (MSCN) method. Munzke et al. [10] combined distributed strain sensing via integrated FOS and acoustic emission. The strain sensing was performed for load cycles until burst of the vessel. While pressurising the vessel material fatigue could be monitored and spatially localized. Critical material changes were detected 17,000 cycles before material failure. The acoustic emission analysis was mainly used for validation, but was also proposed as a suitable tool for the periodic inspection.

In addition to the combined methods, the strain-based Approach can also be used alone. Often distributed FOS are used to monitor the strain distribution over the whole vessel. Kunzler et al. [11] investigated the influence of pressure cycles and impacts by measuring the axial and transverse strain fields with multi-axis fibre grating sensors. Klute et al. [12] embedded a circumferentially-wrapped FOS with a helical pitch along the axis of the composite vessel. The

sensors are interrogated using optical frequency domain reflectometry (OFDR). The distributed strain along circumferentially embedded sensors was measured over a range of pressures before a damage, after a first blunt impact, and after a second blunt impact. The presented configuration provides precise strain distributions as well as it detects and quantifies the occurred defects. Maurin et al. [13] developed complementary criteria based on distributed strain OFDR measurements to propose an efficient and easily understandable SHM procedure for COPV structures.

In previous studies, not related to COPVs, strain-based SHM was utilized with so called Structural Damage Indicators (SDI) [14]. SDIs work with baselines resp. zero references such as strain at the neutral axis of a beam [15] or the zero-strain direction [16]. In the case of a COPV, the known damage indicators cannot be transferred since the dominating load case of internal pressure causes neither a neutral axis nor a zero strain direction. Therefore, a procedure with a strain database is proposed within the scope of this paper. Here, the damage detection works with the comparison of measured values and the database. The strain values in the database are initially generated by values simulated on a FE model. However, they can also be extended by experimentally determined values at a later stage.

3 MODEL AND MODEL REDUCTION TOWARDS THE DIGITAL SHADOW

The modelled COPV is designed for an internal operating pressure of 200 bar. The inner diameter of the vessel is 320 mm, the height (axial) of the cylindrical part is 475 mm. Even though type IV pressure vessels can be operated at inner pressures of up to a 1000 bar [17], the basic construction of COPVs does not change, which is why the vessel modelled here is suitable as a representative COPV model.

3.1 Finite Element Model

The FEM model of the COPV is generated and simulated using Abaqus CAE 2017 [18] supported by a Python interface. Geometrically, the vessel is divided into two spherical dome sections and a cylindrical section, as shown in Figure 1. The model consists of a total of 7,500 full integration four node shell-elements. For the cylindrical part, each element has a size of approx. 10 mm in circumferential direction and 19 mm in axial direction. Here, for monitoring purposes, only the cylindrical area of the COPV is considered in the following. The modelled COPV is approximated with a homogeneous layer structure and thickness over all sections [19]. The vessel is modelled with seven composite plies, whose orientation and thickness are shown in Table 1. The inner liner is not modelled because, it does not have a load-bearing function. The material properties which are used for all layers are given in Table 2.

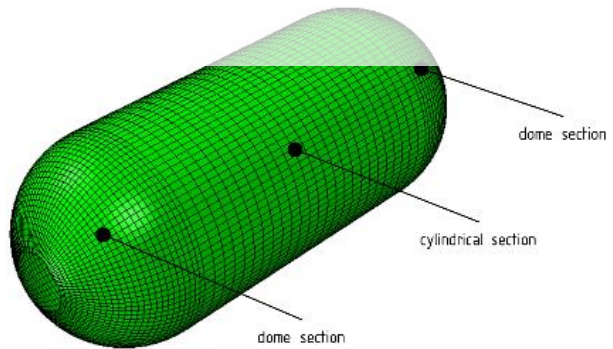


Figure 1: Generated FEM model of the COPV divided into three sections

A static load case is used as test load case. The vessel is loaded with an internal pressure of 100 bar. The load of 100 bar is arbitrary and can be varied within the operating range of the COPV. In the application, the static load case can be achieved, for example, by a short stop during filling.

Table 1: Stacking sequence and layer thickness of the modelled COPV.

Layer	Orientation [°]	Hoop/Helical	Thickness [mm]
Ply 1	88.5	Hoop	1.4
Ply 2	-16.2	Helical	0.9
Ply 3	16.1	Helical	0.9
Ply 4	-25.0	Helical	0.9
Ply 5	88.5	Hoop	1.2
Ply 6	30.0	Helical	1.2
Ply 7	88.5	Hoop	0.6

Table 2: Material properties for Carbon/ Epoxy layers in fibre and perpendicular to fibre direction and for the damaged areas

Carbon/Epoxy Layers	E_1 [MPa]	E_2 [MPa]	ν_{12}	G_{12} [MPa]	G_{13} [MPa]	G_{23} [MPa]
	144838	8098	0.32	3100	3100	1800
Damage	E [MPa]		ν	G [MPa]		
	810		0.32	306		

There is a wide range of safety-critical damages for COPVs [3]. The damage type modelled here is typically triggered by local impacts. The consequence of impact damage is the reduced stiffness of the structure in the impact area [20]. The modelled damage corresponds to matrix cracks with fibre breakage. To model the damage, the fibre is assumed to have no more influence (isotropic material behaviour) and the stiffness is reduced to 10 % of the material properties of the undamaged matrix material (see Table 2). To insert a damage into the model, the damage material properties are assigned to individual elements, also shown in Figure 3.

Register for free at <https://www.scipedia.com> to download the version without the watermark

3.2 Sensor Position and Coverage Analysis

As mentioned above, the information of the model must be reduced to a limited number of measuring points. Therefore, the positioning and the required data point coverage must be set first. The latter is determined in relation to a detectable (minimum) damage size. The first approach aims to find the most sensitive layer to apply or integrate the sensors. Therefore, the strain state of a damaged COPV structure is compared to the one of an undamaged structure. In detail this results in the comparison of the strain values for each element at every section point and in every preselected strain direction.

Table 3: Used Symbols and Indices

Symbol	Description
$\varepsilon\%$	Percentage deviation
M	No. of centroid positions
Indice	Description
11, 22	Strain direction according to the orientation in 11
SP	Section Point; Indicates position in thickness direction
p	Sensor; Indicates global position in COPV
u	Undamaged data
d	Damaged data

First, the difference between the strain values of all section points at all positions of the damaged structure with those of the undamaged structure, is calculated and converted into percentage deviations (see equations (1) and (2)). The used symbols and indices can be found in Table 3.

$$\varepsilon_{11,SP,p}^{\%} = \frac{\varepsilon_{11,SP,p,d} - \varepsilon_{11,SP,p,u}}{\varepsilon_{11,SP,p,u}} \quad (1)$$

$$\varepsilon_{22,SP,p}^{\%} = \frac{\varepsilon_{22,SP,p,d} - \varepsilon_{22,SP,p,u}}{\varepsilon_{22,SP,p,u}} \quad (2)$$

Second, the percentage deviations of the strain values of each section point at each position are compared to each other, to subsequently determine which section point reacts most sensitively in ε_{11} resp. in ε_{22} direction (see equations (4) and (5)). The comparison between these two values indicates the more sensitive direction (see equation (6)).

$$\varepsilon_{11,SP_{max},p}^{\%} \text{ with: } SP_{max} = SP_i \text{ with } \max(\varepsilon_{11,SP_i,p}^{\%}), i \in [1, M] \quad (4)$$

$$\varepsilon_{22,SP_{max},p}^{\%} \text{ with: } SP_{max} = SP_i \text{ with } \max(\varepsilon_{22,SP_i,p}^{\%}), i \in [1, M] \quad (5)$$

$$\varepsilon_{\phi_{max}\phi, SP_{max},p}^{\%} \text{ with } \max(\varepsilon_{11,SP_{max},p}^{\%}; \varepsilon_{22,SP_{max},p}^{\%}) \quad (6)$$

Figure 2 shows the result of the sensor position analysis for the COPV. With the help of the colour distribution and the directions of the arrows, it can be visually determined which layer reacts most sensitively to the induced damage and in which direction the sensors should be positioned in. This evaluation method is not restricted to the COPV and can be applied to different structures with different composite layers and directions.

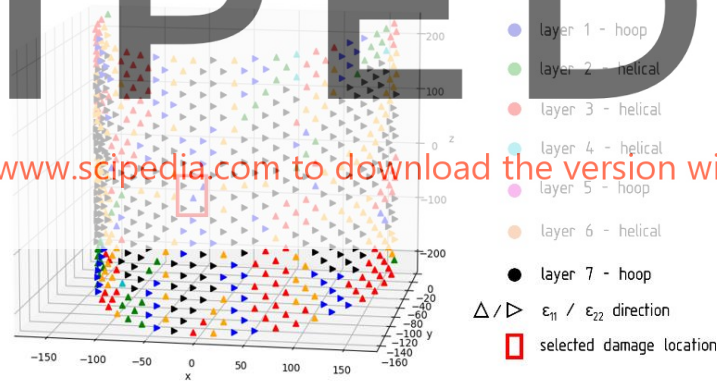


Figure 2: Illustration of the plotted result of the Sensor Position Analysis (for clarity reasons only one half of the cylindrical part is shown).

From a manufacturing point of view, the best solution is to place sensors in only one layer, since the winding process only must be stopped once. For this reason, only one layer is selected here as well. For the considered COPV, the evaluation and comparison of the damaged and undamaged strain state shows the largest percentage deviations in the outermost layer (layer 7, black) perpendicular to the fibre direction (ε_{22} -direction). This result is only a first estimate of the most sensitive layer due to the simplified modelling of the COPV. Nevertheless, the outermost layer has the advantage of placing sensors onto the surface. This reduces the manufacturing complexity and offers the advantage that sensors are accessible to be maintained in case of sensor failure. Thus, monitoring in the outermost layer can help to provide a cost-effective SHM solution. For following considerations, the outermost layer will be selected. Moreover, only strain perpendicular to the fibre orientation ε_{22} will be evaluated.

3.3 Sensor Coverage Analysis

After the orientation and the positioning in the thickness direction have been determined, the next step is to determine the sensor spacing depending on the size of the detectable damage. On the one hand, the number of required sensors should be kept as low as possible to save the costs. Integrating too many sensors means that there is still room to further reduce the system costs. On the other hand, any structural damage must be detectable by the integrated sensors. In case not enough sensors are integrated, potential safety risks can occur, as the structure may fail in an unforeseen way. For this reason, the area of influence is determined for damages of different sizes. Figure 3 shows a damage with the size of 1 element with its area of influence. The farthest points in the area of influence are chosen as sensor positions, each in the circumferential and axial direction. The distances between these points are referred to as the ranges of influence. Table 4 shows the calculated influence ranges for varied induced damage sizes. Using the sensor spacing and the given geometry of the structure, the total number of required sensors is calculated. The results of the sensor coverage analysis in circumferential and axial direction, as well as for the whole vessel, can be displayed in a compact form in a Pareto front, see Figure 4.

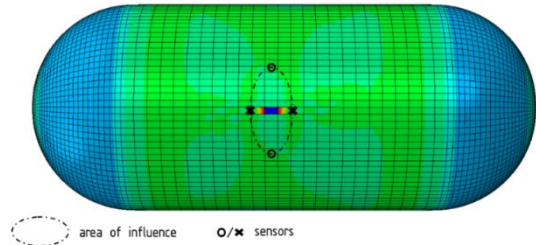


Figure 3: FEM Model of the COPV with a damage sized 10 mm x 19 mm (dark blue) and the corresponding range of influence

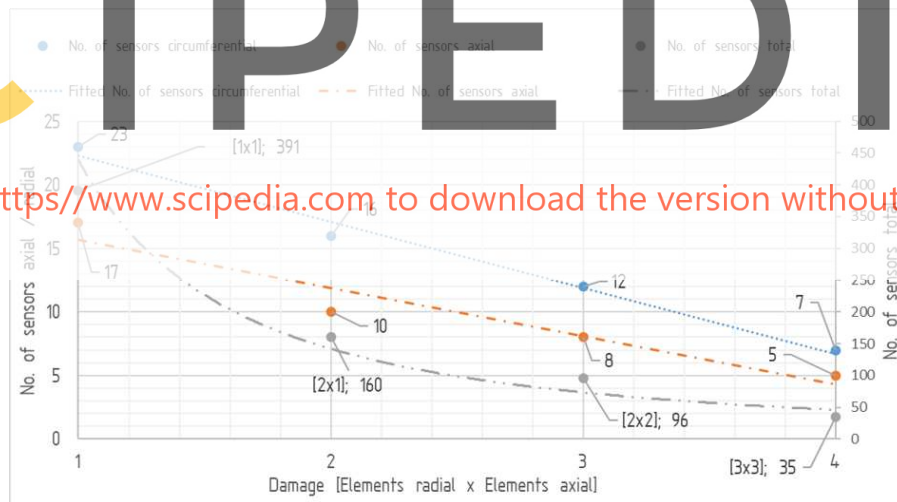


Figure 4: Pareto Front displaying the required number of sensors vs. the damage size to be monitored, damages according to Table 4

Table 4: Tabular overview of the different damage sizes and associated ranges of influence.

Damage	Damage size		Range of damage influence	
	Circumferential [mm]	Axial [mm]	Circumferential [mm]	Axial [mm]
1	10	19	89	57
2	20	19	130	95
3	20	38	168	133
4	30	57	322	200

For the selected damage of the size 2 x 2 elements (damage 3, see Table 4), approx. 96 sensors are required for proper monitoring (see). This corresponds to 12 required sensors in circumferential direction and at least eight required sensors in axial direction. The sensor positions can only be adjusted in element-sized steps. In order to achieve equidistant positioning of the measuring points, only ten sensors each are positioned in the circumferential direction. The mesh resolution in axial direction leads to a selection of alternating eight or nine measuring points, as illustrated in Figure 5.

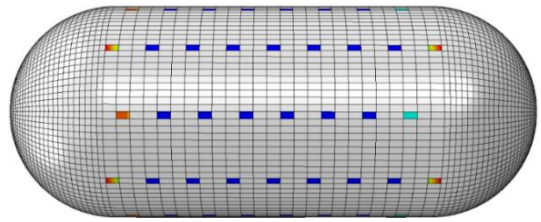


Figure 5: COPV structure reduced to the embedded FBG (strain) sensors, all coloured elements represent sensor

4 SHM SYSTEM

The COPV is digitally represented by single measuring points where only strain information is available. The digital representation of the structure is consequently a simplification of the reality. Therefore, the term Digital Shadow is used for the developed SHM system. The SHM system is divided into two independently functioning subsystems, a damage detection system and a damage assessment system, see Figure 6. According to Rytter's definition [21], the first subsystem is to be understood as a level 1 SHM system, since it only provides a statement about whether there is damage in the structure or not. The second and more powerful subsystem is based on a damage database generated using FEM simulations. By comparing the stored strain values of the database to the measured strain values of the embedded sensors, a SHM system is generated that is classified as a level 3 system. Both subsystems use the same number of embedded sensors.

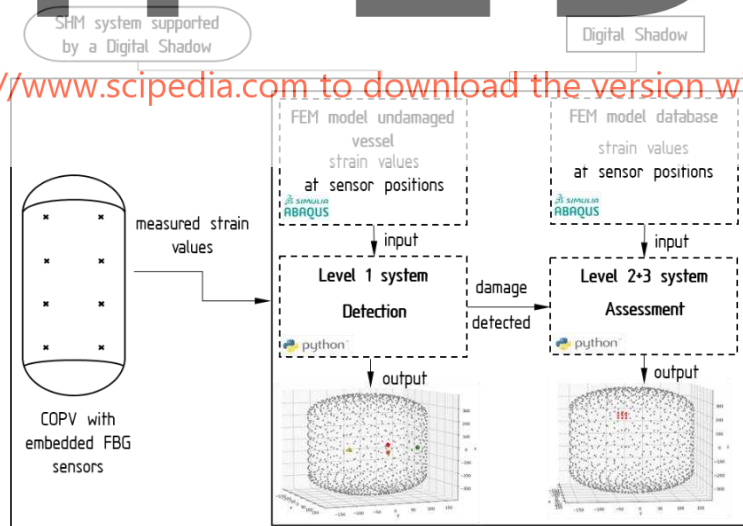


Figure 6: Interaction between the different components of the SHM system

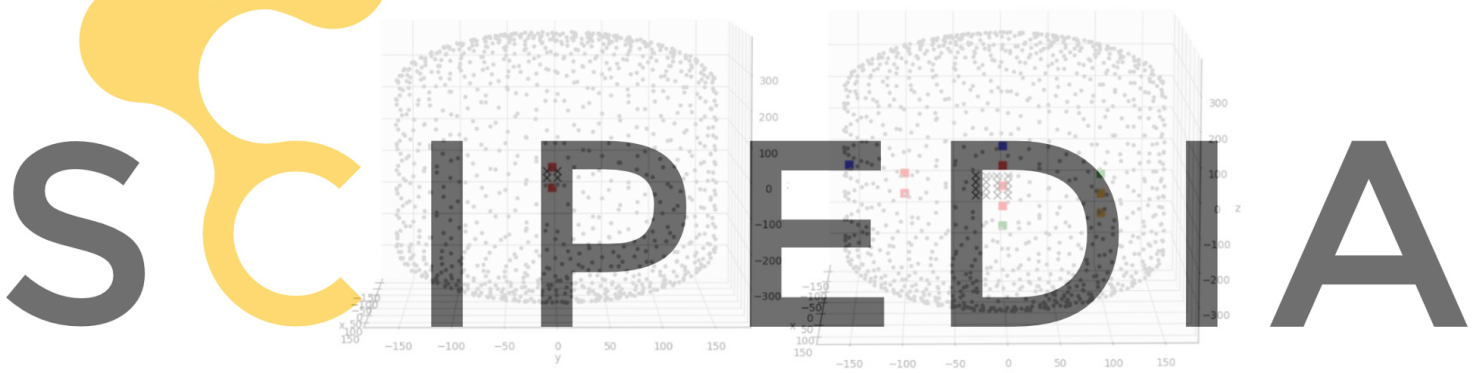
4.1 Level 1 Subsystem: Damage Detection

The Level 1 subsystem is based on the assumption that there is damage in the structure as soon as one or more of the embedded sensors detect a deviation from their initial strain value. The system works similarly to the sensor coverage analysis and is therefore based on the comparison of two strain states of the same structure. The strain values of the sensors are

compared to those of the stored database of an undamaged COPV structure for each sensor p . The differences ($\Delta\varepsilon$) between the strain values of the tested structure (ε_x) and those of the undamaged reference structure (ε_R) are calculated as shown in equation (7) for each sensor p . $\Delta\varepsilon_p$ values below the chosen threshold of $8 \cdot 10^{-5} \varepsilon$ are not considered for further processing. It is assumed that the measured strain values do not match exactly the values stored in the Digital Shadow, which uses the strain values of a FEM simulation, due to possible manufacturing tolerances, sensor positioning or the simplifications made within the model. Therefore, the calibration parameter C_p is introduced. Before the first measurement each sensor will be calibrated with C_p so that $\Delta\varepsilon_p$ is zero in the first place. The calibration parameter gives a constant deviation due to manufacturing errors and a variable deviation with respect to temperature. The determination of the calibration parameter is not the focus of the present work.

$$\Delta\varepsilon_p = \varepsilon_{x,p} - \varepsilon_{R,p} + C_p ; p \in [0, 85] \quad (7)$$

If damage in the COPV is detected, the second subsystem of the SHM system will be triggered, see Figure 7. If no damage is detected in the structure, the inspection process will be terminated and the structure will be used without restrictions.



Register for free at <https://www.scipedia.com> to download the version without the watermark

Figure 7: Results of the Level 1 Damage detection for a small damage (left) and a bigger damage (right); coloured points indicate values greater than the thresholds

4.2 Level 2+3 Subsystem: Localization and Damage Assessment

In order to assess the detected damage from the measured strain state of the COPV, a data-based method is developed. For this purpose, a database with several damages is created. The measured strain state will be compared with the database entries to identify the most reliable damage state.

Creation of the strain state (damage case) database

The strain state database can consist of experimentally determined data, simulated data or a mixture of both. Here, each strain state s is generated by a FEM simulation of the COPV model. The models differ only in position and extent of the applied damage. By continuously shifting the damage in axial and circumferential direction, database entries are generated. Strain states or damages can only be distinguished and thus assessed up to a certain resolution. This resolution is determined by the mesh resolution, since the damage, shown schematically in Figure 8, can only be shifted in the order of scale of the mesh elements. For each damage case s , the strain values of the 85 sensor positions are stored within the database. In addition to the strain and the position information of the sensors, the elements whose material properties are

changed to simulate damage for the respective database entry are also stored. Here the created database consists of a total of 50 damage cases. Half of the damage cases have a size of 2 x 2 elements, the other half a size of 3 x 3 elements.

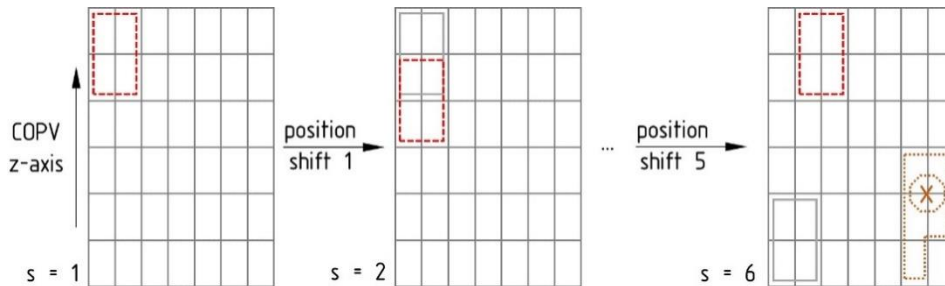


Figure 8: Meandering variation of the damage positions for database creation - illustration of the geometry of the unknown case X

Functionality of the damage assessment subsystem

The damage assessment subsystem compares the measured strain values at each sensor point $\varepsilon_{x,p}$ with those of the stored database values $\varepsilon_{s,p}$. In reality, measurement inaccuracies will always occur, which means that an exact match between the measured value and the database will never be achieved. Instead of requiring the equality of the two strain values, only its similarity is queried, by including an uncertainty parameter ζ . For example, a value of $\zeta = 0.1$ means that the measured strain value on the structure may deviate by up to 10 % from the stored strain value in the database, and the two values are still considered as matched. The magnitude of the permitted uncertainty must be adapted to the specific application.

$$\varepsilon_{x,p} \leq \varepsilon_{s,p} \cdot (1 + \zeta) \quad (8)$$

$$\wedge \varepsilon_{x,p} \geq \varepsilon_{s,p} \cdot (1 - \zeta) \quad (9)$$

For each stored database damage case s , a value i_s is set to $i_s = 0$. If the conditions (8) and (9) are met for a strain value, measured by a sensor p , the value i_s will be increased by 1. This process is repeated for all sensors p . The resulting value i_s is divided by the total number of sensors and multiplied by 100. The resulting percentage value is stored as percentage match value m_s . These steps are repeated for all stored damage cases s in the database. Once this process has been executed for all s , the maximum match value m_s is determined. The measured strain state thus matches the strain state most closely, which has the largest value m_s . The damage that occurred at the real COPV is therefore assessed as the damage that was inserted to the FEM model of the COPV for this database entry. The developed match algorithm can be further improved by adapting the arithmetic mean of all measured strain values on a z-coordinate due to the rotationally symmetrical geometry of the vessel. As soon as one of the strain values deviates more than the standard deviation, its region must be assumed to be damaged.

Test case: Distinction of the most similar strain states

The first test examines if a stored database damage will be recognised despite the uncertainty parameter ζ . The damage case 16 (2x2) is selected. For the uncertainty parameter ζ the value $\zeta = 0.1$ is set. As shown in Figure 9, a 100% match is achieved for the expected damage case 16 (2x2, grey). For the selected parameter $\zeta = 0.1$, it is also possible to sufficiently and precisely distinguish between the stored strain states, since no other database

entry achieves such a high match m_s . It is thus shown that the developed algorithm fulfils its function and damage assessment will be possible, if the damage occurring at the COPV is already stored in the database.

Test case: Assessment of an unknown damage case

The assumption is made that no damage occurring at the COPV causes the exact same strain state as a previously simulated damage. This in turn means that no 100% match is achieved for a stored damage case, as it is the case in the previous test performed. In order to evaluate how well an unknown damage case can be assessed by the system, a strain state is therefore, used as the measured state at the COPV, which is not stored in the database. The damage marked with an X in Figure 8 with 5 damaged elements is used as the unknown damage case. The strain state of the unknown damage is compared with the available database damage using the equations 8 and 9. For a selected uncertainty factor of $\zeta = 0.1$ the results are shown in Figure 10. No match m_s of 100% is determined for a stored damage case. This is the expected result, as the assessed damage is not known. The highest value of m_s is reached for the damage case 7 (2x2). However, the damage cases 1, 2 and 7 (3x3) result in an equally large value of m_s . Consequently, no assessment or precise localisation of the unknown damage is possible.

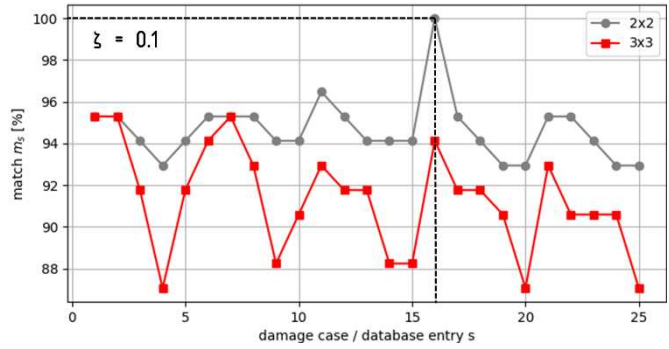


Figure 10: Result of the damage assessment for a known damage - illustration of the match m_s - grey: 2x2 damages, red: 3x3 damages

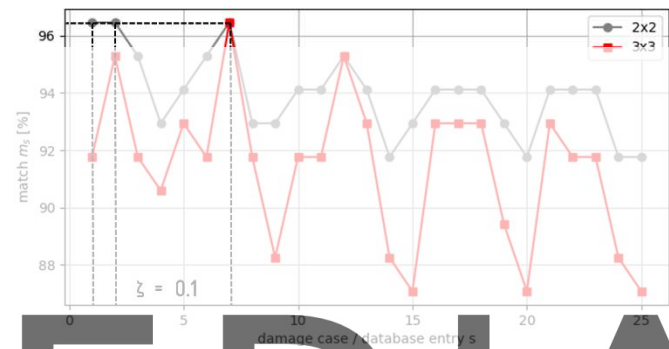


Figure 9: Result of the damage assessment for an unknown damage - illustration of the match m_s - grey: 2x2 damages, red: 3x3 damages

S C I P E D I A

Register for free at <https://www.scipedia.com> to download the version without the watermark

No match m_s of 100% is determined for a stored damage case. This is the expected result, as the assessed damage is not known. The highest value of m_s is reached for the damage case 7 (2x2). However, the damage cases 1, 2 and 7 (3x3) result in an equally large value of m_s . Consequently, no assessment or precise localisation of the unknown damage is possible.

To further evaluate the damage assessment algorithm the variable e_s (element match) is introduced. e_s indicates how many elements of the unknown damage case and determined database entry are equal, see Figure 11. For damage case 7 (2x2), e_s has the value 0/5. This means the damage is incorrectly localised by the damage assessment subsystem. For the damage case 7 (3x3), the value e_s is equal to 2/5. In general, the best results that can be achieved are $e_s = 4/5$ for 2x2 damages or $e_s = 5/5$ for 3x3 damages.

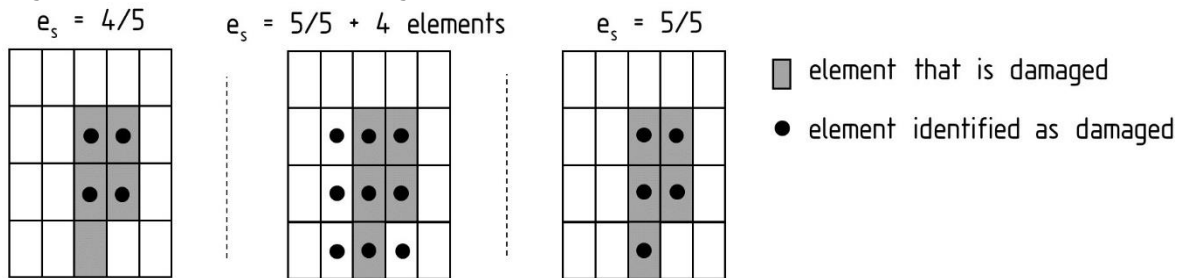


Figure 11: Illustration of the element match parameter e_s , left: damage is assessed as too small, middle: damage is assessed as too large, right: potential optimum, not reachable by developed algorithm

5 CONCLUSIONS

This work demonstrates the approach of an SHM System supported by a Digital Shadow. To realise these system requirements, the most sensitive sensor positions are determined at first. Furthermore, an analysis method is created to decide on the quantity of sensors needed for monitoring, depending on the induced damage. The SHM system consists of two independently functioning subsystems that differ in their performance and complexity. The first subsystem is used for level 1 damage detection. The system is based on comparing the sensor values measured at the COPV with those of an undamaged FEM model of the same structure. The second subsystem is used for level 2+3 damage assessment and localisation. It determines the most similar strain state to the measured one from a database of strain states considering uncertainties. If a damage case is already stored in the database, it can be exactly assessed and localised. Even unknown damage that is similar to a database entry can be assessed by the algorithm. However, as soon as damages occur at the COPV that differ significantly from the ones stored in the database, an assessment is no longer possible. Nevertheless, the damage detection is unaffected by that issue, leading to a successful damage detection.

The presented algorithm shows good results. Probably, the database matching can be made faster and more robust using pattern recognition methods as well as machine learning approaches. In the long term, it would make sense to supplement the database with experimentally determined data in addition to the simulated references. This makes the system less dependent on the previously generated FE data and would automatically expand the database to include several types of damage.

REFERENCES

- [1] A. G. Olabi, T. Wilberforce und M. A. Abdelkareem, „Fuel cell application in the automotive industry and future perspective,“ *Energy*, Bd. 214, 2021.
- [2] P. B. McLaughlan, S. C. Forth und L. R. Grimes-Ledesma, „Composite Overwrapped Pressure Vessels (COPV), A Primer,“ *National Aeronautics and Space Administration (NASA)*, 2011.
- [3] P. McKeon, A Fundamental Study to Enable Ultrasonic Structural Health Monitoring of a Thick-Walled, Composite, Over-Wrapped-Pressure Vessel, PhD thesis: Georgia Institute of Technology, 2014.
- [4] ASTM International, *E2533-09: Standard Guide for Nondestructive Testing of Polymer Matrix Composites Used in Aerospace Applications*, 2009.
- [5] T. Huang und K.-U. Schröder, „A Hybrid Damage Detection Method for Composite Pressure Vessel,“ *21st International Conference on Composites Materials*, 2017.
- [6] A. Güemes, A. Fernandez-Lopez, A. R. Pozo und J. Sierra-Pérez, „Structural Health Monitoring for Advanced Composite Structures: A Review,“ *J. Compos. Sci. (Journal of Composites Science)*, Bd. 4, Nr. 1, 2020.
- [7] W. Zhou, Z. Wu und L. Mevel, „Vibration-based Damage Detection to the Composite Tank Filled with Fluid,“ *Structural Health Monitoring*, Bd. 9, Nr. 5, pp. 433 - 445, 2010.
- [8] M. Bocian, M. Panek, D. Pyka und N. Alexandre, „Vibration Analysis of High Pressure Composite Carbon Fiber Vessels Subjected to Mechanical Impact,“ in *Advanced*

- Materials for Defense*, Switzerland, Springer, 2020, p. 103–110.
- [9] T. Huang und K.-U. Schröder, „A HYBRID DAMAGE DETECTION SYSTEM FOR COMPOSITE PRESSURE VESSEL,“ in *21st International Conference on Composite Materials*, Xi'an, China, 2017.
- [10] D. Munzke, E. Duffner, R. Eisermann, M. Schukar, A. Schoppa, M. Szczepaniak, J. Strohacker und G. Mair, „Monitoring of type IV composite pressure vessels with multilayer fully integrated optical fiber based distributed strain sensing,“ *Materials Today: Proceedings*, Bd. 34, pp. 217 - 223, 2021.
- [11] M. Kunzler, E.Udd, M. Johnson und K.Mildenhall, „Approved for Public Release, Distribution is Unlimited Use of Multidimensional Fiber Grating Strain Sensors for Damage Detection in Composite Pressure Vessels,“ *Proceedings of Smart Structures and materials*, Bd. Vol. 5788, pp. 83 - 92, 2005.
- [12] S. M. Klute, D. R. Metrey, N. Garg und N. A. A. Rahim, „In-situ structural health monitoring of composite overwrapped pressure vessels,“ *SAMPE Journal*, Bd. 52, Nr. 2, pp. 7 - 17, 2016.
- [13] L. Maurin, P. Ferdinand, F. Nony und S. Villalonga, „OFDR Distributed Strain Measurements for SHM of Hydrostatic Stressed Structures: An Application to High Pressure Hydrogen Storage Type IV Composite - H2E Project,“ in *EWSHM - 7th European Workshop on Structural Health Monitoring*, Université de Nantes, Nantes, France, 2014.
- [14] A. Preisler, „Efficient Damage Detection and Assessment Based on Structural Damage Indicators,“ PhD Thesis, RWTH Aachen University, Aachen, 2019.
- [15] A. Preisler, K.-U. Schröder und M. Schagerl, „Intrinsic Damage Assessment of Beam Structures Based On Structural Damage Indicators,“ *American Journal of Engineering Research (AJER)*, Bd. 7, Nr. 6, p. 56–70, 2018.
- [16] A. Preisler und K.-U. Schröder, „Ein interdisziplinärer Ansatz zur intelligenten FKV-Welle,“ in *4SMARTS 2017 Symposium für Smarte Strukturen und Systeme*, Braunschweig, Germany, 21./22. Juni 2017.
- [17] R. Moradi und K. Groth, „Hydrogen storage and delivery: Review of the state of the art technologies and risk and reliability analysis,“ *International Journal of Hydrogen Energy*, Bd. 44, Nr. 23, 2019.
- [18] Dassault Systèmes, *Abaqus CAE*, 2017.
- [19] A. Reynaldo, H. Pramono, S. Santosa und M. Aziz, „Finite Element Analysis of Liquefied Ammonia Tank for Mobility Vehicles Employing Polymers and Composites,“ *Energies*, Bd. 13, 2020.
- [20] S. P. Rajbhandari, M. L. Scott, R. S. Thomson und D. Hachenberg, „An approach to modelling and predicting impact damage in composite structures,“ in *ICAS 2002: 23rd International Congress of Aeronautical Sciences*, Toronto, 2002.
- [21] A. Rytter, *Vibrational Based Inspection of Civil Engineering Structures*, PhD Thesis, University of Aalborg, 1993.
- [22] A. Barrias, J. R. Casas und S. Villabla, „A Review of Distributed Optical Fiber Sensors for Civil Engineering Applications,“ *Sensors*, Bd. 16, Nr. 5, 2016.